ORIGINAL ARTICLE

Korean J Orthod 2005:35(5):388-97

Formulation of a reference coordinate system of three-dimensional (3D) head & neck images: Part I. Reproducibility of 3D cephalometric landmarks

Jae-Woo Park, DDS, MSD,[a] Nam-Kug Kim, MS,[b] Young-Il Chang, DDS, MSD, PhD[c]

The purpose of this study was to redefine the cephalometric landmarks in three-dimensional (3D) images, which are used in orthodontic cephalometric radiography, and to evaluate the reproducibility of each landmark for 3D cephalometric analysis. Eighteen CT scans were taken at the Department of Diagnostic Radiology at Seoul National University Dental Hospital and manipulated with V works 4.0 (Cybermed Inc., Seoul, Korea). The coordinate system was established using 7 reference points, with no more than 4 points on the same plane. These 7 points were generated as a volume model, the voxel size of which was 4 by 4 by 2 (threshold value = 639). The cephalometric landmarks were selected at the multiplanar reformation (MPR) window on the volume mode of V works 4.0. The selected landmarks were exported to V surgery (Cybermed Inc., Seoul, Korea) for the calculation of coordinate values. All the data were taken twice with a lapse of 2 weeks by one investigator. The reproducibility of each landmark was 0.17~1.21 mm in the x axis, 0.30~1.53 mm in the y axis, and 0.27~1.81 mm in the z axis. In all three axes, the range of error was similar. These error ranges were acceptable with regards to the pixel space and slice thickness. The most reproducible points were I points which were selected on the basis of the volume model. The least reproducible points were J points that were defined by sutures.

(**Key words**: 3D landmark, Reproducibility, Reference coordinate system)

[a] Graduate Student, [c] Professor, Department of Orthodontics, School of Dentistry and Dental Research Institute, Seoul National University

[b] Graduate Student, Department of Industrial Engineering, College of Engineering, Seoul National University

*Reprint requests: **Nam-Kug Kim***

Department of Industrial Engineering, Seoul National University, Sillim-Dong, Gwanak-Gu, Seoul 151-742, Korea

+82 11 9073 4282 / cyberrog@kornet.net

Received March 10, 2005; Last Revision May 17, 2005; Accepted May 19, 2005

INTRODUCTION

Orthodontics is that branch of dentistry concerned with the study of facial growth, occlusal development, and the treatment of dentofacial abnormalities in a three-dimensional (3D) aspect. Broadbent suggested the cephalometric radiograph for 3D analysis of the dentofacial complex with bipolar images.[1] Since then, many authors have suggested their own analyses to

diagnose dental and/or facial deformities and establish treatment planning.[2] Ironically, all of these efforts were concentrated to lateral cephalometric analysis, which confined orthodontic analysis to a two-dimensional (2D) analysis of projected images rather than an actual 3D analysis of reality.

Baumrind et al.[3,4] suggested paired coplanar radiography using frontal and lateral cephalometric radiographs to overcome these shortcomings. Grayson et al.[5] and Bookstein et al.[6] tried 3D analysis with biplanar images. Brown and Abbott[7] demonstrated how to obtain 3D coordinate values of landmarks with a photogrammetric equation, taking cephalometric radiographs from one X-ray source.

Kusnoto et al.[8] invented a specially designed face bow to obtain P-A, lateral, and submentovertex views. They suggested that data could be easily collected from each view, and were clinically comparable to CT data. But the images obtained from this method were merely some polygons in the form of a mesh, not the real 3D images.

Recently, with the increased need for orthognathic surgery and an extended application of the surgical technique for treatment of dentofacial deformities, some limitations have been encountered in the diagnosis and treatment planning with 2D analysis. Therefore the clinical application of 3D images has gradually increased.

Some authors have introduced the use of 3D models from CT scans for treating patients with severe dentofacial deformity or facial asymmetry. Fuhrmann et al.[9] and Fuhrmann[10] showed that in treating patients with facial asymmetry, better results were obtained from the use of a polyurethane foam model combined with the study cast for surgical planning. Karcher[11] combined the 3D CT model and study cast with the use of a miniscrew as a reference marker. This was used as a lifesized model during treatment.

Hsieh et al.[12] developed a surgical simulator with the CT data. Xia et al.[13-15] also developed a 3D surgical simulator for orthognathic surgery, which could confirm the surgical results 3-dimensionally by mapping the facial contour to the simulated results. Carls et al.[16] insisted that the 3D CT can visualize facial anatomy in certain patients such as those with asymmetries, large defects, and fractures with major dislocation, and that this assimilated information allow for a more accurate evaluation. But, CT protocols are less indicated because of higher levels of radiation. In the near future, radiation dose will be greatly reduced with the development of cone beam CT, which can extend the use of CT scans in orthognathic surgery.[17,18]

Three-dimensional images can allow a detailed overview of the topographic relations between dento-maxillofacial structures in all planes of space from any viewpoint without superimposition of any anatomic structures. CT images can also make it possible to study biologic variation, morphologic dimensions, or biologic processes etc. Waitzman et al.[19] tried to define normal values for a series of craniofacial measurements and to evaluate the growth patterns of the craniofacial complex through CT. Maki et al.[20] investigated 3D distribution of bone mineralization in the developing mandible. They also tried to investigate the possible association between bone shape and cortical bone mineral density in asymmetrical mandibles.[21]

But in all of these studies, 3D images were used to compare the size of the left and right sides. Moreover, the landmark selection was arbitrarily accomplished, so the results could not be quantified and were not comparable. So the application of 3D medical images was not able to catch up with the technical development.

The purpose of this study was to redefine the cephalometric landmarks used in orthodontic cephalometric radiography, and to evaluate the reproducibility of each landmark for 3D cephalometric analysis.

MATERIAL AND METHODS

Sample selection

CT scans were taken from 18 patients who attended Seoul National University Dental Hospital for orthognathic surgery. Eight were male, and the rest were female. CT data acquisition was carried out using a Somatom Plus 4 (Siemens, Erlangen, Germany) at a

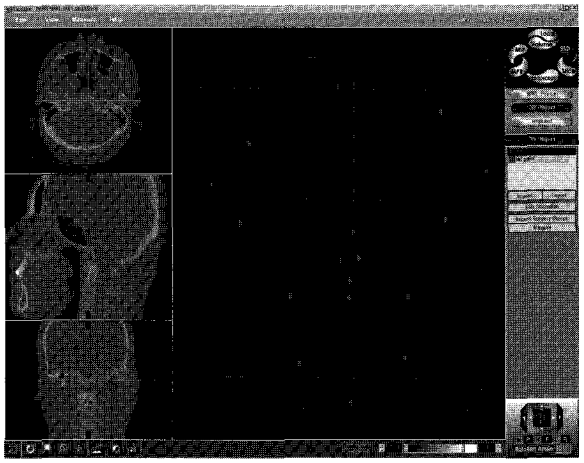

Fig 1. Volume model rendering for reference points and I points.

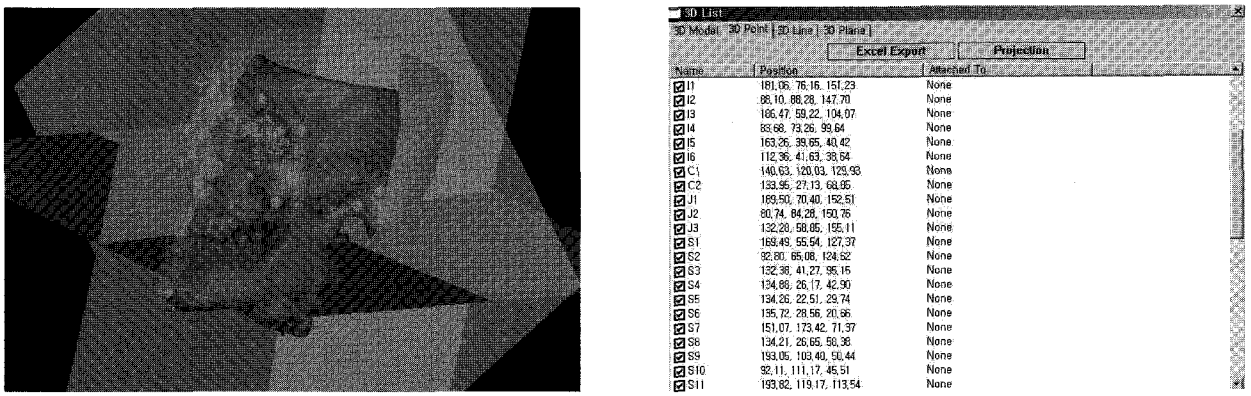

Fig 2. Project file creation and extraction of coordinate values.

1.5 mm section interval, a 1 mm slice thickness in the spiral mode, and a 512 by 512 matrix. The scans were carried out at the Department of Diagnostic Radiology of Seoul National University Hospital. The resultant 2D image data were stored in Digital Imaging and Communications in Medicine (DICOM) format.

Programs used to set reference points: V works 4.0 and V surgery

V works 4.0 (Cybermed Inc., Seoul, Korea) was used to select the 3D landmarks. Seven reference points were isolated as a volume model of 4 by 4 by 2 pixel size. The threshold value for isolation was 865. These points were used to establish common coordinate systems (Fig 1). Three points out of 7 were used for a horizontal reference plane. One point and the midpoint of 2 points out of the other 4 points were used for the sagittal plane. The last point was used for the coronal plane and as zero point of the coordinate system. These 3 planes are perpendicular to each other. All these procedures are described in the next paragraph. After the selection of 3D landmarks, project files were exported to V surgery (Cybermed Inc., Seoul, Korea) to extract the coordinate values (Fig 2).

Establishment of the coordinate system

Seven reference points were selected near the anatomic structures listed below. The order of coordinate system setting was as follows;

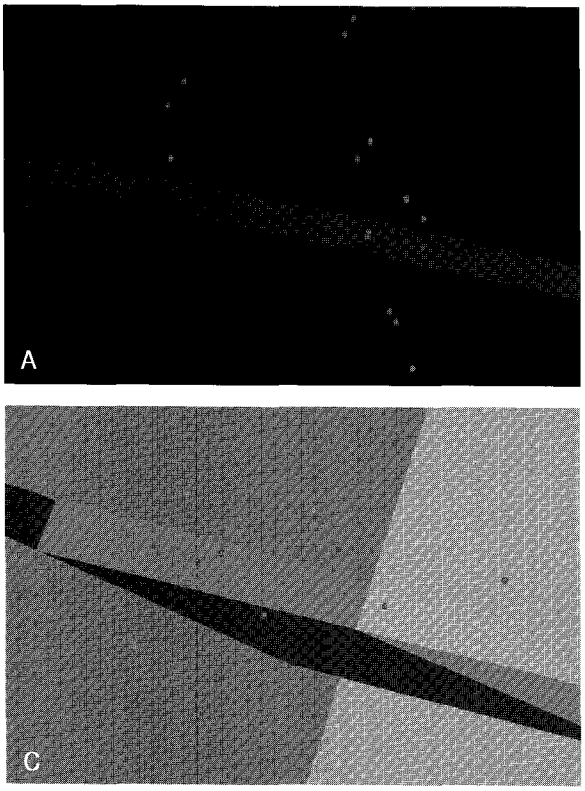

Fig 3. Establishment of the common coordinate system. **A**, Creation of the horizontal plane; **B**, creation of the mid-sagittal plane; **C**, creation of the coronal plane.

a > Configurations for the horizontal plane (Fig 3, *A*)
R1: mesiobuccal cusp of left maxillary molar; R2: mesiobuccal cusp of right maxillary molar; R3: Incision Superius.
b > Configurations for the sagittal plane (Fig 3, *B*)
The sagittal plane was established to include point R4 and the midpoint of R5 and R6, perpendicular to the horizontal plane.
R4: Prosthion; R5: apex of left maxillary central incisor; R6: apex of right maxillary central incisor.
c > Configurations for the coronal plane (Fig 3, *C*)
The coronal plane was established to include R7 point, perpendicular to the horizontal plane and sagittal plane.
R7: Basion.

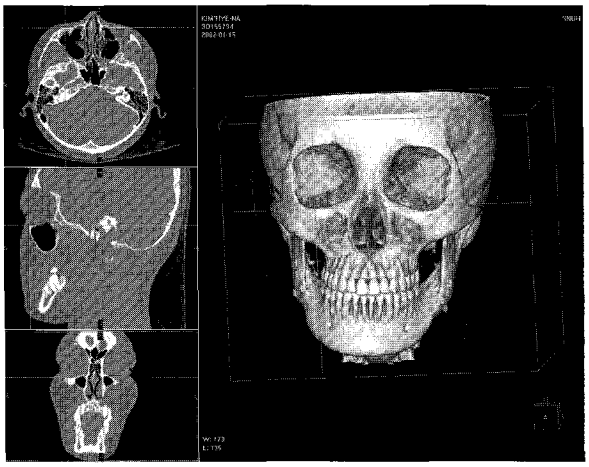

Fig 4. Picking the volume point in the MPR mode.

Selection of 3D landmarks (Fig 4)

Three-dimensional landmarks were defined as V points and grouped according to their positions in the 3D model and named as follows. Odd numbers were given to the left sided landmarks, even numbers were given to the right sided landmarks;

a > I point: The point selected on the basis of the

volume model to indirectly investigate the reproducibility of reference points. The volume model was generated around the following anatomic structures with the same conditions as the reference points.

I1/I2: frontomalar suture Lt/Rt; I3/I4: Key ridge; Lt/Rt; I5/I6: Mental foramen Lt/Rt.

b > J point: The points positioned at the junction of sutures (3 points).

J1/J2: Frontomalar suture Lt/Rt; The most supero-lateral suture point between malar bone and frontal bone; J3: Nasion; The junction of the nasal and frontal bones as seen on the profile of the cephalometric radiograph; point in the midline of both the nasal root and the nasofrontal suture.

c > S point: The points positioned on the surface or line angle of the bone (18 points).

S1/S2: Orbitale Lt/Rt; The lowest point on the lower margin of each orbit; S3: A point; The deepest midline point on the premaxilla between anterior nasal spine and prosthion; S4: B point; The most posterior point of the bony curvature of the mandible below infradentale and above pogonion; S5: Pogonion; The most anterior point on the symphysis of the mandible; S6: Menton; The lowest median landmark on the lower border of the mandible-concave surface under the mentum in the mid-sagittal plane; S7: Opisthion; The most posterior point on the posterior margin of foramen magnum; S8: Infradentale; The most antero-superior point on the mandibular alveolar process between the mandibular central incisors; S9/S10: Gonion Lt/Rt; The point on the bony contour of the gonial angle determined by bisecting the tangent angle; S11/S12: Condylion Lt/Rt; The most postero-superior point on the condyle; S13/S14: Condylion Medialis Lt/Rt; The most medial point of the condylar head, intersected with the long axis of the condylar head; S15/S16: Condylion Lateralis Lt/Rt; The most lateral point of the condylar head, intersected with the long axis of the condylar head; S17: Incision Superius; The midpoint of the incisal edge of the maxillary central incisor; S18: Incision Inferius; The midpoint of the incisal edge of the mandibular central incisor.

d > F point: The points defined by foramina (12 points).

F1/F2: Foramen Spinosum Lt/Rt; The geometric center of foramen spinosum which can be found in the most inferior horizontal section; F3/F4: Foramen Supraorbitale Lt/Rt; midpoint of the notch appearing in the superior margin of the orbital rim; F5/F6: Foramen Infraorbitale Lt/Rt; The midpoint of the orifice of the infraorbital foramen; F7/F8: Porion Lt/Rt; The midpoint on the upper edge of porus acusticus externus; F9/F10: Foramen Ovale; The most inferior point in the latero-posterior margin of foramen ovale; F11/F12: Foramen Rotundum; The geometric center of foramen rotundum which can be found in the most anterior coronal section.

e > P point: The points positioned at the end of the bony projection (12 points).

P1: Nc; The most superior point of crista galli, the projection of the perpendicular lamina of the ethmoid; P2: Rhinion; The most antero-inferior point on the tips of the nasal bones as seen from norma lateralis; P3: ANS; The most anterior point of the nasal floor; tip of premaxilla; P4: PNS; The most posterior point on the hard palate; P5/P6: L1 Apex Lt/Rt; The root tip of the mandibular central incisor; P7/P8: Clinoidale Lt/Rt; The most posterior point on the contour of the anterior clinoid; P9/P10: Coronoid process; The most superior point on the coronoid process; P11/P12: U6 Lt/Rt; The mesiobuccal cusp tip of the maxillary 1st molar.

f > C point: The center of sella turcica (sella)

g > O point: Zero point defined by the coordinate system

Reproducibility

One orthodontist selected the cephalometric landmarks twice on the same CT data with a lapse of 2 weeks. The coordinate values of each landmark were obtained. The differences in coordinate values were calculated. Mean, standard deviation (SD), and standard error (SE) of the differences were calculated to evaluate the reproducibility of the landmarks.

RESULTS

Table 1 shows the data of each group. The reproducibility of O point showed axis dependence,

Table 1. Reproducibility of grouped landmarks

	X axis		*Y axis*		*Z axis*	
	Mean ± SD	*SE*	*Mean ± SD*	*SE*	*Mean ± SD*	*SE*
O point	- 0.01 ± 0.45	0.31	- 0.09 ± 0.32	0.23	- 0.30 ± 1.12	0.80
R point	- 0.01 ± 0.37	0.26	0.05 ± 0.39	0.28	- 0.29 ± 1.05	0.76
I point	- 0.02 ± 0.49	0.34	- 0.05 ± 0.78	0.58	- 0.19 ± 0.87	0.64
V point	- 0.01 ± 0.84	0.58	- 0.02 ± 0.94	0.66	- 0.12 ± 1.19	0.83
J point	- 0.13 ± 1.37	0.97	- 0.28 ± 1.67	1.19	- 0.06 ± 1.83	1.28
S point	- 0.04 ± 0.80	0.57	0.07 ± 0.82	0.58	- 0.08 ± 1.20	0.85
F point	0.08 ± 0.90	0.64	- 0.14 ± 0.91	0.54	- 0.13 ± 1.27	0.90
P point	- 0.01 ± 0.62	0.43	0.04 ± 0.85	0.60	- 0.18 ± 0.88	0.63
C point	- 0.19 ± 0.86	0.61	- 0.27 ± 0.97	0.69	0.05 ± 0.72	0.49

Table 2. Reproducibility of reference points

	X axis		*Y axis*		*Z axis*	
	Mean ± SD	*SE*	*Mean ± SD*	*SE*	*Mean ± SD*	*SE*
R1	- 0.02 ± 0.30	0.21	0.08 ± 0.50	0.35	- 0.30 ± 1.12	0.80
R2	0.03 ± 0.34	0.23	0.10 ± 0.38	0.27	- 0.30 ± 1.12	0.80
R3	- 0.01 ± 0.41	0.28	0.09 ± 0.38	0.27	- 0.30 ± 1.12	0.80
R4	- 0.01 ± 0.45	0.31	0.02 ± 0.35	0.24	- 0.41 ± 1.19	0.87
R5	- 0.01 ± 0.46	0.31	- 0.03 ± 0.43	0.29	- 0.40 ± 1.10	0.81
R6	0.00 ± 0.45	0.31	0.03 ± 0.41	0.29	- 0.30 ± 1.19	0.85
R7	- 0.02 ± 0.13	0.09	0.09 ± 0.32	0.23	0.01 ± 0.36	0.25

which was 0.31 in the x axis, 0.23 in the y axis, and 0.80 in the z axis. It was inferred that this resulted from the difference between the pixel space (< 0.5 mm) and the slice thickness (1 mm). This tendency was also seen in the reproducibility of reference points and I points which showed larger errors in the z axis than in the x and y axis.

The reproducibility of V points were 0.58 in the x axis, 0.66 in the y axis, and 0.83 in the z axis. These error ranges were acceptable with regards to the pixel space and slice thickness. But, J point, which was defined by the sutures, showed larger errors than any of the other points.

The mean, SD, and SE of each point are shown in Table 2 to Table 7. Points R1, R2, and R3, which were used to define the horizontal plane, showed the same errors in the z axis. Points R4, R5, and R6, which were used to define the mid-sagittal plane, showed the same errors in the x axis (Table 2). Compared with R points, I points showed increased errors in the x and y axes, and a decreased error in the z axis (Table 3).

J points showed the largest error in all three axes. On the contrary, C point, which was defined as the center of sella turcica, showed relatively good reproducibility (Table 4). Of all the points positioned on the surface or line angle of the bone, S1 and S2 showed large errors in the x axis, S10 in the y axis, and S4, S5, S9, and S10 in the z axis. The points defined in the condyle head showed good reproducibility (Table 5). The points defined by foramina

Table 3. Reproducibility of I points

	X axis		*Y axis*		*Z axis*	
	Mean ± SD	*SE*	*Mean ± SD*	*SE*	*Mean ± SD*	*SE*
I1	- 0.06 ± 0.65	0.45	- 0.17 ± 1.04	0.72	- 0.11 ± 0.63	0.44
I2	0.01 ± 0.69	0.47	- 0.15 ± 0.97	0.68	- 0.12 ± 0.67	0.47
I3	- 0.05 ± 0.48	0.33	- 0.11 ± 0.54	0.38	- 0.23 ± 0.80	0.57
I4	- 0.01 ± 0.43	0.29	- 0.01 ± 0.43	0.30	- 0.27 ± 0.92	0.66
I5	- 0.03 ± 0.39	0.27	0.16 ± 0.85	0.59	- 0.29 ± 1.02	0.73
I6	0.00 ± 0.23	0.16	0.13 ± 0.70	0.49	- 0.29 ± 1.14	0.81

Table 4. Reproducibility of O, J, and C points

	X axis		*Y axis*		*Z axis*	
	Mean ± SD	*SE*	*Mean ± SD*	*SE*	*Mean ± SD*	*SE*
O point	- 0.01 ± 0.45	0.31	- 0.09 ± 0.32	0.23	- 0.30 ± 1.12	0.80
J1	- 0.55 ± 1.33	1.00	- 0.36 ± 1.66	1.17	- 0.46 ± 1.17	0.99
J2	0.22 ± 1.57	1.09	- 0.22 ± 2.22	1.53	- 0.25 ± 1.17	0.83
J3	- 0.06 ± 1.14	0.78	- 0.24 ± 1.00	0.71	0.52 ± 2.58	1.81
C point	- 0.19 ± 0.86	0.61	- 0.27 ± 0.97	0.69	- 0.05 ± 0.72	0.49

Table 5. Reproducibility of S points

	X axis		*Y axis*		*Z axis*	
	Mean ± SD	*SE*	*Mean ± SD*	*SE*	*Mean ± SD*	*SE*
S1	- 0.45 ± 1.70	1.21	- 0.30 ± 0.93	0.67	- 0.37 ± 1.03	0.75
S2	0.04 ± 1.74	1.19	- 0.15 ± 1.04	0.72	- 0.28 ± 1.08	0.77
S3	- 0.23 ± 0.45	0.35	- 0.10 ± 0.53	0.37	- 0.40 ± 1.26	0.91
S4	- 0.03 ± 0.49	0.34	- 0.12 ± 0.63	0.44	0.01 ± 1.72	1.18
S5	- 0.13 ± 0.61	0.43	0.27 ± 0.84	0.61	0.27 ± 1.51	1.05
S6	- 0.09 ± 0.36	0.25	0.05 ± 1.13	0.78	- 0.45 ± 1.32	0.96
S7	0.23 ± 0.86	0.61	0.21 ± 0.72	0.51	- 0.11 ± 0.91	0.63
S8	- 0.07 ± 0.43	0.30	0.20 ± 0.55	0.40	- 0.44 ± 1.36	0.99
S9	- 0.28 ± 0.85	0.62	0.50 ± 0.98	0.76	- 0.24 ± 1.62	1.13
S10	0.08 ± 0.70	0.49	0.28 ± 1.63	1.14	0.11 ± 2.15	1.48
S11	0.18 ± 0.94	0.66	0.31 ± 0.73	0.54	0.11 ± 0.58	0.41
S12	- 0.47 ± 0.84	0.67	0.04 ± 0.63	0.44	0.16 ± 0.56	0.40
S13	0.00 ± 0.25	0.17	-0.18 ± 0.53	0.39	0.05 ± 0.86	0.59
S14	0.05 ± 0.29	0.20	0.03 ± 0.46	0.32	0.29 ± 0.93	0.67
S15	0.06 ± 0.27	0.19	0.00 ± 0.69	0.48	0.00 ± 0.72	0.50
S16	- 0.13 ± 0.29	0.22	- 0.06 ± 067	0.46	0.17 ± 0.77	0.54
S17	0.19 ± 0.60	0.44	0.06 ± 0.58	0.40	- 0.32 ± 1.32	0.93
S18	0.28 ± 0.59	0.45	0.19 ± 0.39	0.30	- 0.02 ± 0.74	0.51

Table 6. Reproducibility of F points

	X axis		*Y axis*		*Z axis*	
	Mean ± SD	*SE*	*Mean ± SD*	*SE*	*Mean ± SD*	*SE*
F1	0.07 ± 0.43	0.30	- 0.08 ± 0.60	0.42	- 0.15 ± 1.14	0.79
F2	- 0.04 ± 0.37	0.26	- 0.17 ± 0.43	0.32	- 0.27 ± 1.37	0.96
F3	0.08 ± 1.03	0.71	- 0.26 ± 1.47	1.03	- 0.43 ± 1.13	0.84
F4	0.12 ± 1.19	0.82	- 0.23 ± 1.26	0.88	- 0.38 ± 1.20	0.86
F5	0.03 ± 0.74	0.51	- 0.20 ± 0.83	0.59	- 0.47 ± 1.09	0.82
F6	- 0.01 ± 0.70	0.48	- 0.19 ± 0.79	0.56	- 0.35 ± 0.94	0.69
F7	- 0.15 ± 1.14	0.79	- 0.01 ± 0.84	0.58	0.01 ± 1.24	0.86
F8	0.32 ± 0.91	0.67	- 0.09 ± 0.76	0.53	- 0.07 ± 0.86	0.59
F9	0.22 ± 0.62	0.45	- 0.12 ± 0.76	0.53	0.14 ± 0.69	0.48
F10	- 0.12 ± 0.47	0.33	- 0.30 ± 0.86	0.63	- 0.14 ± 0.79	0.55
F11	- 0.21 ± 0.99	0.70	0.07 ± 1.11	0.77	0.30 ± 1.55	1.08
F12	0.61 ± 1.45	1.09	- 0.09 ± 0.98	0.68	0.21 ± 2.41	1.66

Table 7. Reproducibility of P points

	X axis		*Y axis*		*Z axis*	
	Mean ± SD	*SE*	*Mean ± SD*	*SE*	*Mean ± SD*	*SE*
P1	- 0.05 ± 0.73	0.51	- 0.19 ± 1.30	0.90	- 0.22 ± 0.60	0.44
P2	0.01 ± 0.69	0.47	- 0.46 ± 0.99	0.75	- 0.70 ± 1.13	0.92
P3	0.03 ± 0.96	0.66	- 0.26 ± 0.55	0.42	- 0.37 ± 1.41	1.00
P4	- 0.04 ± 0.95	0.65	0.43 ± 0.55	0.48	- 0.16 ± 0.60	0.42
P5	- 0.08 ± 0.44	0.31	0.15 ± 0.54	0.38	- 0.22 ± 1.28	0.89
P6	0.06 ± 0.40	0.28	0.21 ± 0.55	0.41	- 0.20 ± 1.14	0.79
P7	0.06 ± 0.46	0.32	- 0.32 ± 0.98	0.71	- 0.25 ± 0.56	0.42
P8	0.02 ± 0.44	0.30	- 0.16 ± 0.97	0.67	- 0.08 ± 0.38	0.27
P9	0.03 ± 0.50	0.34	0.08 ± 0.81	0.56	- 0.04 ± 0.70	0.48
P10	- 0.13 ± 0.59	0.42	0.04 ± 0.61	0.42	- 0.17 ± 0.90	0.63
P11	0.06 ± 0.55	0.38	0.52 ± 0.82	0.67	- 0.06 ± 0.46	0.32
P12	- 0.10 ± 0.51	0.36	0.43 ± 0.74	0.59	0.29 ± 0.66	0.50

showed acceptable reproducibility with a tendency that the more definite the canal observed in the MPR mode, the more accurate the identification (Table 6). The points positioned at the end of the bony projection showed smaller errors in the z axis than in the x or y axis, which had an opposite tendency from the otherpoints. Of course the errors in the x and y axes were also small (Table 7).

DISCUSSION

The reproducibility of O point was absolutely dependent on the reproducibility of R points used to define the coordinate system. And the R points showed axis dependence, which meant the error of the z axis showed larger errors than those of the x and y axes. This tendency was reflected in the repro-

ducibility of O points, 0.31 in the x axis, 0.23 in the y axis, and 0.80 in the z axis. It was inferred that this resulted from the difference between the pixel space (< 0. 5mm) and the slice thickness (1 mm).

The reproducibility of R points was very accurate, but by definition, some points had the same coordinate value in a specific axis. For example, the z coordinates of points R1, R2, and R3 were the same, and the x coordinates of points R4, R5, and R6 were the same. Since this might decrease the error of each point, it was reasonable that the reproducibility of R points should be inferred from that of I points. The reproducibility of I points were 0.34 in the x axis, 0.58 in the y axis, and 0.64 in the z axis, which were relatively accurate. This meant it was very stable to set the coordinate system using the landmarks marked by voxels.

Despite the difference between the pixel space and slice distance, the reproducibility of volumetric landmarks showed a similar range of errors in all three axes, 0.17 ~ 1.21 in the x axis, 0.30 ~ 1.53 in the y axis, and 0.27 ~ 1.81 in the z axis. This might be because the large slice thickness would make more apparent changes in the anatomical structure around some landmarks, which made a more accurate selection possible. One other plausible cause might be that the large z axis error of O point could mask the z axis error of other volumetric points. The contribution of each cause could not be discriminated in this study. This might be made possible after the development of a program which could export the DICOM coordinate directly in the near future.

The reproducibility of each landmark did not show an apparent difference according to the position in the 3D model. This might be because the landmarks were selected in the MPR mode, not in the volume model. So the coordinate values of landmarks which could be apparently defined in the MPR mode showed smaller errors, and vice versa. This made a large difference in the reproducibility of each axis in the same landmark.

Generally, the landmark defined by the sutures could not be defined as a point or angular point in the MPR mode. So the reproducibility was relatively low. The other landmarks defining a point or angular point in the MPR mode showed a relatively small error. C point defined as the center of sella turcica showed a unique high reproducibility in spite of not being defined on the volume model, especially in the z axis.

CONCLUSIONS

Cephalometric landmarks used for orthodontic diagnosis are only 2D projections of 3D anatomical structures. This might evoke a projection error as even the earliest investigators have known. Although the projection error could not lower the diagnostic value of orthodontic cephalometry, it might be meaningful to define the 3D landmarks and investigate the reproducibility of the landmarks to seek the anatomical truth in the oral and maxillofacial area. The reproducibility of each landmark was 0.17 ~ 1.21 in the x axis, 0.30 ~ 1.53 in the y axis, and 0.27 ~ 1.81 in the z axis, all three axes showed similar ranges of error. These error ranges were acceptable with regards to the pixel space and slice thickness. It was thought that the reproducibility of the landmarks was determined mainly according to the degree of demarcation in the MPR mode, not the position in the volume model. The most reproducible points were I points which were selected on the basis of the volume model. The least reproducible points were J points which were defined by the sutures.

- 국문초록 -

3차원 두부영상의 기준좌표계 설정을 위한 연구: I부 CT영상에서 3차원 계측점의 재현성

박재우 · 김남국 · 장영일

이 연구는 기존의 두부방사선사진에서 사용되었던 계측점들을 3차원으로 재구성한 CT자료에서 다시 정의하고, 그 점들의 재현도를 조사함으로써, 재현성이 높고 해부학적 특징을 잘 표현하는 점들을 제안하고자 시행하였다. 3차원 영상에서 상대적 좌표값을 구하기 위해 어느 4점도 같은 평면에 존재하지 않는 7개의 고정점을 선정하여 기준 좌표계를 설정하였다. V works 4.0 (Cybermed Inc., Seoul, Korea)을 이용하여 고정점과 I점 설정을 위한 volume model (voxel size = 4·4·2, threshold value = 639)을 형성한 후 계측점을 선택하였으며, 나머지 점들은 모두 volume mode의 MPR 창을

이용하여 선정하였다. 이렇게 선정한 계측점을 V surgery (Cybermed Inc., Seoul, Korea)로 이출하여 각 점의 상대적 공간 좌표값을 구하였다. 모든 자료는 2주 간격으로 2번 측정한 후 재현도를 계산하였다. 각 계측점의 재현도는 x축 0.13 ~ 1.24 mm, y축 0.23 ~ 1.53 mm, z축 0.15 ~ 1.81 mm로 유사한 범위를 보였다. 재현도가 우수한 것은 고정점을 이용한 I점이며 봉합에 의해 정의되는 J점의 재현도가 비교적 낮게 나타났다.

(**주요 단어**: 3차원 계측점, 재현도, 기준좌표계)

REFERENCES

1. Broadbent BH. A new x-ray technique and its application to orthodontia. Angle Orthod 1931;1:1-45.
2. Proffit WR, Ackerman JL. Orthodontic diagnosis: The development of a problem list. In: Proffit WR ed. Contemporary orthodontics. St Louis: Mosby; 2000. p. 170-85.
3. Baumrind S, Moffitt FH, Curry S. Three-dimensional x-ray stereometry from paired coplanar images. A progress report. Am J Orthod 1983;84:292-312.
4. Baumrind S, Moffitt FH, Curry S. The geometry of three-dimensional measurement from paired coplanar x-ray images. Am J Orthod 1983; 84:313-22.
5. Grayson B, Cutting C, Bookstein FL, Kim H, McCarthy JG. The three-dimensional cephalogram: theory, technique, and clinical application. Am J Orthod Dentofacial Orthop 1988;94:327-37.
6. Bookstein FL, Grayson B, Cutting CB, Kim HC, McCarthy JG. Landmarks in three dimensions: reconstruction from cephalogram versus direct observation. Am J Orthod Dentofacial Orthop 1991;100:133-40.
7. Brown T, Abbott AH. Computer-assisted location of reference points in three dimensions for radiographic cephalometry. Am J Orthod Dentofacial Orthop 1989;95:490-8.
8. Kusnoto B, Evans CA, BeGole EA, de Rijk W. Assessment of 3-dimensional computer-generated cephalometric measurements. Am J Orthod Dentofacial Orthop 1999;116:390-9.
9. Fuhrmann RA, Frohberg U, Diedrich PR. Treatment prediction with three-dimensional computer tomographic skull models. Am J Orthod Dentofacial Orthop 1994;106:156-60.
10. Fuhrmann RA. Three-dimensional cephalometry and three-dimensional skull models in orthodontic/surgical diagnosis and treatment planning. Semin Orthod 2002;8:17-22.
11. Karcher H. Three-dimensional craniofacial surgery: transfer from a three-dimensional model (Endoplan) to clinical surgery: a new technique (Graz). J Craniomaxillofac Surg 1992;20:125-31.
12. Hsieh MS, Tsai MD, Chang WC. Virtual reality simulator for osteotomy and fusion involving the musculoskeletal system. Comput Med Imaging Graph 2002;26:91-101.
13. Xia J, Wang D, Samman N, Yeung RW, Tideman H. Computer-assisted three-dimensional surgical planning and simulation: 3D color facial model generation. Int J Oral Maxillofac Surg 2000;29:2-10.
14. Xia J, Ip HH, Samman N, Wang D, Kot CS, Yeung RW, et al. Computer-assisted three-dimensional surgical planning and simulation: 3D virtual osteotomy. Int J Oral Maxillofac Surg 2000;29: 11-7.
15. Xia J, Samman N, Yeung RW, Wang D, Shen SG, IP HH, et al. Comupter-assisted three-dimensional surgical planning and simulation. 3D soft tissue planning and prediction. Int J Oral Maxillofac Surg 2000;29:250-8.
16. Carls FR, Schuknecht B, Sailer HF. Value of three-dimensional computed tomography in craniomaxillofacial surgery. J Craniofac Surg 1994;5: 282-8.
17. Vannier MW. Craniofacial computed tomography scanning: technology, applications and future trends. Orthod Craniofacial Res 2003;6 Suppl 1:23-30.
18. Sukovic P. Cone beam computed tomography in craniofacial imaging. Orthod Craniofacial Res 2003;6 Suppl 1:31-6.
19. Waitzman AA, Posnick JC, Armstrong DC, Pron GE. Craniofacial skeletal measurements based on computed tomography: part II Normal values and growth trends. Cleft Palate Craniofac J 1992;29:118-28.
20. Maki K, Miller AJ, Okano T, Shibasaki Y. A three-dimensional, quantitative computed tomographic study of changes in distribution of bone mineralization in the developing human mandible. Arch Oral Biol 2001;46:667-78.
21. Maki K, Miller AJ, Okano T, Hatcher D, Yamaguchi T, Kobayashi H, et al. Cortical bone mineral density in asymmetrical mandibles: a three-dimensional quantitative computed tomography study. Eur J Orthod 2001;23:217-32.